Journal of Hazardous Materials 178 (2010) 434–439

Contents lists available at ScienceDirect

Journal of Hazardous Materials

journal homepage: www.elsevier.com/locate/jhazmat

Dye removal from aqueous solution by magnetic alginate beads crosslinked with epichlorohydrin

Vincent Rocher[a,b,c], Agnès Bee[a,b,c,*], Jean-Michel Siaugue[a,b,c], Valérie Cabuil[a,b,c]

[a] UPMC Univ Paris 06, UMR 7195, Laboratoire Physicochimie des Electrolytes, Colloïdes et Sciences Analytiques (PECSA), Case 51, 4 place Jussieu, F-75005 Paris, France
[b] CNRS, UMR 7195, Laboratoire Physicochimie des Electrolytes, Colloïdes et Sciences Analytiques (PECSA), F-75005 Paris, France
[c] ESPCI, UMR 7195, Laboratoire Physicochimie des Electrolytes, Colloïdes et Sciences Analytiques (PECSA), F-75005 Paris, France

ARTICLE INFO

Article history:
Received 25 June 2009
Received in revised form
18 December 2009
Accepted 20 January 2010
Available online 25 January 2010

Keywords:
Adsorption
Magnetic separation
Alginate
Ferrofluid
Activated carbon
Methylene blue
Methyl orange

ABSTRACT

Innovative magnetic alginate beads are used to remove organic pollutants from aqueous solution under different experimental conditions. These alginate beads (EpiMAB) are prepared by an extrusion technique and crosslinked with epichlorohydrin. They contain both magnetic nanoparticles and activated carbon (AC). With the addition of magnetic properties, the beads can be easily recovered or manipulated with an external magnetic field. Their capacity to adsorb pollutants is linked to encapsulated AC and to active sites coming from both magnetic nanoparticles and alginate. The efficiency of the beads as biosorbent for the removal of dyes is assessed using methyl orange (MO) and methylene blue (MB) as model molecules. The dye uptake is found to vary with the initial concentration and the charge of the adsorbed molecule. The Langmuir equation fits well the adsorption data with maximum adsorption capacities of 0.02 mmol/g for MO and 0.7 mmol/g for MB. Kinetics experiments are performed to evaluate the equilibrium time; the pseudo-second-order kinetic model adequately describes the experimental data. The influence of the pH of the solution on adsorption is also investigated and a comparison with alginate beads crosslinked by calcium ions is made.

1. Introduction

Various techniques are being used to remove pollutants from aqueous waste, with sorption being one of the most promising technologies for water purification. The most used adsorbents are clay minerals [1,2], activated carbon [3] and polymers [4,5]; there is also a growing interest in the use of biomaterials such as polymers obtained from renewable resources due to their availability and ease of employment [6–8]. Activated carbon (AC) is a widely used sorbent in water purification processes, owing to its high adsorption capacity coming from its large surface area and porous structure. However, AC is mostly used as a fine powder: the difficulty of separating it from the effluent may result in the loss of the sorbent.

The encapsulation of AC into alginate beads is an elegant solution to overcome this problem. Alginate is a natural polysaccharide extracted from brown seaweed. It has many advantages such as availability, low cost, non-toxicity, biocompatibility and biodegradability, and is also an efficient biosorbent due to the presence of carboxylate functions along its chains. Recently, composite sorbents like AC-encapsulating alginate beads have attracted some attention because they combine the properties and advantages of each of their components.

Magnetic nanoparticles are also encapsulated alongside AC within the alginate beads to produce a magnetic sorbents easily recovered using a magnet. Such magnetic sorbents are being investigated by researchers more and more [9–12].

The adsorption properties of the alginate beads containing magnetic nanoparticles and AC presented in this study are assessed by using two organic dyes as models of pollutants: positively charged methylene blue and negatively charged methyl orange. Such dyes are also pollutants themselves: used in a lot of industries (textile, paper, food, etc.), their presence in the effluents reduces light penetration and photosynthesis, while some dyes prove toxic or carcinogenic: this makes their removal an important challenge [10–12].

In our previous work, magnetic alginate beads containing AC powder were prepared with a simple process: the materials to be encapsulated (magnetic nanoparticles and AC) were mixed with a sodium alginate solution and dropped into a calcium solution resulting in an instantaneous formation of Ca-reticulated alginate beads. These beads are used immediately without drying: the water still present within them precludes any long-term storage. Although effective in their adsorption role, the beads have long

* Corresponding author at: UMR 7195-UPMC, Laboratoire Physicochimie des Electrolytes, Colloïdes et Sciences Analytiques (PECSA), Case 51, 4 place Jussieu, F-75005 Paris, France. Tel.: +33 1 44 27 30 98; fax: +33 1 44 27 32 28.
E-mail address: agnes.bee@upmc.fr (A. Bee).

0304-3894/$ – see front matter © 2010 Elsevier B.V. All rights reserved.
doi:10.1016/j.jhazmat.2010.01.100

equilibration time: around 3 h. This point is to be improved to let them be used in an industrial water treatment process. In this work, we propose a new way to synthesize alginate magnetic beads to solve these problems: starting from Ca-alginate beads, we crosslink alginate with epichlorohydrin. Through this way, we obtain beads with larger pores even after drying, with faster adsorption kinetics and an overall decrease of the time to reach the adsorption equilibrium.

2. Experimental

2.1. Materials

Alginate is a linear polymer composed of β-D-mannuronate (M) and α-L-guluronate (G) units linked by β-1,4 and α-1,4 glycosidic bonds. M and G units are organized in MM, GG and MG blocks, the proportion of these blocks varying with the source of the polymer. Sodium alginate powder was purchased from Fluka. The weight average molar weight (M_w), the number average molar weight (M_n) and the ratio M/G are equal to 1.73×10^5 g/mol, 9.65×10^4 g/mol and 0.90, respectively, average molar weights were determined by gel permeation chromatography. The sodium content of alginate directly related to the number of its carboxylate functions was obtained by atomic absorption spectrophotometry ($[Na]_{alg} = 4.44 \pm 0.23$ mmol/g).

Activated carbon was purchased from Sigma–Aldrich. The surface area and the total pore volume are equal to $1400 \pm 20\ m^2/g$ and 0.64 mL/g, respectively (data supplied by Sigma–Aldrich). The particles are smaller than 149 μm (100 mesh).

The magnetic material used was a ferrofluid composed of roughly spherical maghemite (γ-Fe_2O_3) nanoparticles coated by citrate ions and dispersed in an aqueous solution. Particles were synthesized according to Massart's method described in previous papers [13,14]. The typical mean diameter of the particles and standard deviation are respectively equal to 7.5 nm and 0.36. The amount of sodium counterions of the adsorbed citrate ($[Na]_{mnp}$), obtained by atomic absorption spectrophotometry, is equal to 0.45 mmol/g of maghemite. The maximum surface charge density can be estimated from this characterization and is equal to $29\ \mu C/cm^2$.

Epichlorohydrin (3-chloro-1,2-epoxypropane) with a purity of 99% was purchased from Fluka.

The two dyes, purchased from Sigma–Aldrich, are methylene blue ($C_{16}H_{18}N_3S^+Cl^-$, noted MB) and methyl orange ($C_{14}H_{14}N_3O_3S^-Na^+$, noted MO).

2.2. Synthesis of magnetic alginate beads

Epichlorohydrin-reticulated magnetic alginate beads (EpiMAB) were prepared starting from magnetic Ca-alginate beads (CaMAB). CaMAB were obtained according to the method described in our previous work [15]. 3.0 g of sodium alginate were dissolved in 300 mL of a diluted ferrofluid suspension ([Fe] = 0.333 mol/L), 0.3 g of AC powder was then added to the mixture. After 90 min of mechanical stirring, the suspension was added dropwise into a $CaCl_2$ solution (400 mL, 0.5 mol/L). Beads were left 12 h in the Ca bath before being washed with distilled water 3 times. They were then kept in water or dried at 70 °C in an oven.

Chemically crosslinked alginate beads were obtained following a procedure adapted from Fundueanu et al. [16] and Delval et al. [8]. First, 186 ± 4 g CaMAB were immersed into three consecutive ethanol/water baths (60% v/v in ethanol, 400 mL each) during 2 h each to exchange the water contained in the beads with ethanol. The beads were then put into 400 mL of an ethanol/water solution (60% v/v of ethanol) containing epichlorohydrin (6.109 g). A NaOH solution (1 mol/L) was then slowly added to reach pH ≈ 13. The crosslinking reaction was allowed to proceed for 4 h. The beads were then washed in three consecutive distilled water baths (600 mL each for 2 h). Concentrated HNO_3 solution (53.7% w/w) was added to the last bath to neutralize the mixture (pH ≈ 7). The beads were collected afterwards, weighted and dried for 2 days in an oven at 70 °C.

To perform the kinetics and adsorption experiments, several syntheses of beads were realized. For the syntheses corresponding to samples called EpiMAB-1, EpiMAB-2 and EpiMAB-4, quantities of precursor materials used are close. The alginate, AC and maghemite amounts are equal to (in mg/g of dried beads) 265 ± 19; 27 ± 1 and 709 ± 62, respectively. On the other hand the sample called EpiMAB-3 contains 10 times more AC than the others samples.

2.3. Bead characterization

The quantity of element M in the beads (M = Fe, Na or Ca) was determined by atomic absorption spectrophotometry using a Perkin Elmer AAnalyst 100.

The mean diameter and the size distribution of the beads were obtained from digitized photographs of the beads in combination with image analysis software (ImageJ).

2.4. Adsorption experiments

Batch adsorption equilibrium experiments were performed to study the adsorption process. A known weight of dried beads (0.37 ± 0.05 g) was added into 20 mL of a dye solution at a known initial concentrations (C_0). After shaking the samples for 48 h with an orbital shaker, the beads were magnetically removed from the solution. The equilibrium concentration of dye remaining in the solution (C_{eq}) was determined by UV–vis spectrophotometry using a Varian Cary 50 at 680, 660 and 640 nm for MB and 500, 460 and 420 nm for MO; the corresponding extinction coefficients (ε) were determined with solutions of known concentration beforehand. The amount of adsorbed dye Q_{eq} (in mmol per gram of dried beads) was obtained using the equation:

$$Q_{eq} = \frac{C_0 - C_{eq}}{m} \times V \quad (1)$$

where V (in L) represents the volume of the solution and m (in g) the mass of dry beads; C_0 and C_{eq} are expressed in mmol/L. The Fe, Na and Ca concentrations in the solution ($[M]_s$) were measured by atomic absorption spectrophotometry. The amount of cations remaining into the beads ($[M]_b$) after dye adsorption was calculated from the difference between $[M]_s$ and the initial concentration within the beads ($[M]_i$).

For kinetic experiments, the samples were prepared by adding a known weight of beads (0.36 ± 0.1 g for dried beads and 6.5 ± 0.5 g for wet beads) into a 20 mL solution of dye with the initial concentration C_0 = 1 mmol/L. Zero time was taken when adding the adsorbent to the solution. The samples were shaken with an orbital shaker and taken at appropriate time intervals.

3. Results and discussion

3.1. Bead characterization

The beads are dark due to the ferrofluid and AC encapsulation and roughly spherical. The mean diameter and standard deviation of dry EpiMAB-1 obtained from size histograms fitted with a Gaussian distribution are equal to 1.3 mm and 0.16, respectively.

The element M (M = Fe, Ca or Na) content of the beads is reported in Table 1 for the different bead syntheses. $[M]_i$ and $[M]_f$ represent the concentrations of the cations into the beads after synthesis and

Table 1
Cations present in the beads for different beads preparations (in mmol/g).

Reference	CaMB[a]	EpiMB-1	EpiMB-2	EpiMB-3[b]	EpiMB-4
$[Ca^{2+}]_i$	1.16	0.94	0.73	0.71	0.77
$[Ca^{2+}]_f$	1.01	0.93	0.71	0.69	0.69
$[Na^+]_i$	0	0.34	0.63	0.69	0.11
$[Na^+]_f$	0	0.12	0.12	0.19	0.07
$[Fe]_i = [Fe]_f$	10.0	8.7	9.2	8.0	8.8
$[Fe]_a$	10.4	9.2	8.7	7.6	8.9
$2[Ca^{2+}]_f + [Na^+]_f$	2.0	2.0	1.6	1.6	1.6
$[Na^+]_{alg} + [Na^+]_{mnp}$	1.9	1.5	1.5	1.3	1.6

[a] The values reported were obtained in a previous work [15].
[b] In this synthesis, 10 times more AC were introduced in the beads.

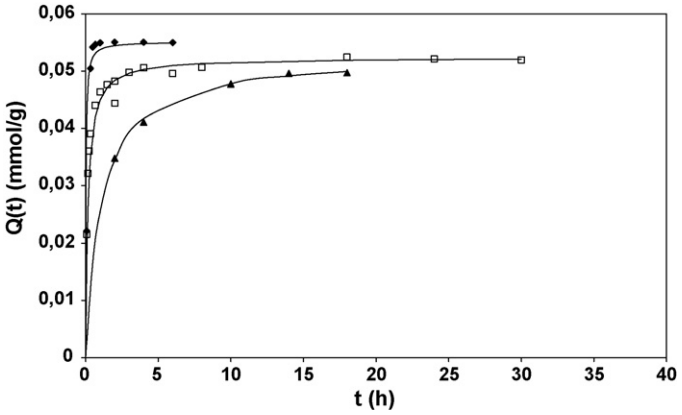

Fig. 1. Adsorption kinetics of MB (C_0 = 1 mmol/L) onto: (▲) dry CaMB, (□) wet CaMB and (♦) dry EpiMB-1. The solid lines represent the fit with a pseudo-second-order equation.

remaining into the beads left for 48 h in distilled water, respectively. The following remarks can be made from the values reported in Table 1: (1) $[Fe]_i \approx [Fe]_f$: no magnetic nanoparticles release occurs when beads are left 48 h in distilled water. Also, $[Fe]_i$ is close to the amount of encapsulated ferrofluid in alginate beads (designated as $[Fe]_a$ in Table 1): no magnetic nanoparticles release occurs during beads preparation. Furthermore, (2) for CaMAB, all the sodium ions are exchanged by calcium ions during the reticulation process; (3) for EpiMAB, due to the use of sodium hydroxide during the reticulation step, Na^+ ions are present in a non-negligible fraction after bead synthesis, but most of them are released in the solution when beads are left 48 h into water. On the other hand, few Ca^{2+} ions are released in solution for the EpiMAB, contrary to CaMAB; (4) the sum $(2[Ca^{2+}]_f + [Na^+]_f)$ is close to the amount of negative charges present in the beads roughly estimated from sodium content of both alginate and magnetic nanoparticles ($[Na^+]_{alg} + [Na^+]_{mnp}$). This sum represents an estimate amount of potential exchangeable cations for adsorption of the dyes.

3.2. Kinetic studies

Fig. 1 shows the results of experiments of methylene blue (MB) adsorption (C_0 = 1 mmol/L) onto wet CaMAB, dry CaMAB and dry EpiMAB-1. By increasing the contact time, the amount of adsorbed MB (Q_t) rapidly increases. Characteristic times corresponding to 50% (t_{50}) and 95% (t_{95}) of the maximum adsorption and amounts of MB adsorbed at equilibrium (Q_{eq}) are reported in Table 2. The experimental values of Q_{eq}, close to 0.05 mmol/g, are quite similar for the three sorbents. On the other hand, the contact time to reach 95% adsorption was shorter for dry EpiMAB-1 and wet CaMAB (30 and 60 min, respectively) than for dry CaMAB (20 h). Two opposite phenomena could explain this result: (1) the drying of the beads decreases their porosity; the structural barrier thus created limits the diffusion of pollutants to the binding sites for adsorption; (2) the crosslinking of alginate with epichlorohydrin, increases the distance between the alginate chains, resulting in a faster adsorption of the pollutants even in the dry state. Dry EpiMAB-1 presents similar properties than wet CaMAB. The characteristics of the both beads are in agreement with comparable studies on adsorption by encapsulated materials [17–19].

A pseudo-second-order equation [20] was used to model the experimental data. This equation is often successfully used to describe the adsorption kinetics of pollutants onto an adsorbent. The pseudo-second-order equation is

$$\frac{dQ_t}{dt} = k(Q_{eq} - Q_t)^2 \quad (2)$$

where k (in g/mmol/min) is the second-order rate constant, Q_{eq} (mmol g^{-1}) the amount of dye adsorbed at equilibrium and Q_t (mmol/g) the amount of dye adsorbed at time t. Integrating the above equation between $t = 0$ and $t = t_{eq}$ and applying boundary conditions $Q(0) = 0$ and $Q(t_{eq}) = Q_{eq}$ gives

$$\frac{t}{Q_t} = \frac{1}{kQ_{eq}^2} + \frac{1}{Q_{eq}}t \quad (3)$$

The kinetic parameters and correlation coefficient are reported in Table 1. The plots of t/Qt versus t yield straight lines and the correlation coefficient R^2 are all equal to 0.999. This confirms that the sorption process obeys to the pseudo-second-order model. The constant k is equal to 1653 g/mmol/min. The equilibrium sorption capacities ($Q_{eq,calc}$) show a good agreement with the experimental value ($Q_{eq,exp}$) and a good fit of the experimental curve is observed (Fig. 1).

The time evolution of the amounts of Na^+ and Ca^{2+} ions within the beads during the adsorption process is reported in Fig. 2. It has to be noticed that the Na^+ and Ca^{2+} quantities into the beads at equilibrium are close to the values obtained after beads were introduced 48 h in distilled water without MB (Table 1). At this stage, it means either that no ionic exchange occurs between cations and adsorbed MB or that, due to the relatively small quantity of MB initially added, this ionic exchange is masked by release in solution of cations, non-associated to the negative charges of the beads.

It has to be noticed that for the following batch adsorption experiments, contact time will be 48 h, which is more than sufficient to establish equilibrium.

3.3. Adsorption isotherms

The adsorption isotherms of MB and MO performed with dry EpiMAB-2 and non-encapsulated AC are plotted in Fig. 3. These isotherms describe equilibrium between adsorbed dye concentra-

Table 2
Kinetic parameters for adsorption of MB (C_0 = 1 mmol/L) onto alginate beads.

Beads	t_{50} min	t_{95} min	$Q_{eq,exp}$ mmol/g	$Q_{eq,calc}$ mmol/g	k g mmol^{-1} h^{-1}	R^2
Wet CaMB[a]	10	60	0.052	0.052	115	0.999
Dry CaMB	60	1200 (20 h)	0.050	0.053	18	0.999
Dry EpiMB-1	10	30	0.055	0.055	700	0.999

[a] The values reported were obtained in a previous work [15].

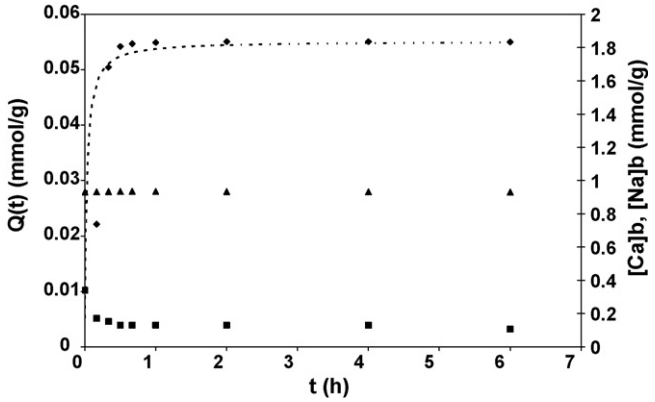

Fig. 2. Adsorption kinetics of MB onto EpiMB-1 (C_0 = 1 mmol/L): (♦) $Q(t)$; (■) $[Na^+]_b$; (▲) $[Ca^{2+}]_b$. The dashed line represents the fit with a pseudo-second-order rate equation.

tion (Q_{eq}) in mmol per gram of dry beads (noted mmol/g) and concentration of dye remaining in solution (C_{eq}) in mmol/L at constant pH. It has to be noted that to compare the sorption capacity of the two adsorbents, Q_{eq} is expressed in mmol per gram of AC (noted mmol/g_{AC}).

The equilibrium adsorption data were fitted by the classical Langmuir equation. The Langmuir model is based on the assumption that all adsorption sites are identical. Although this model cannot provide any mechanistic understanding of the sorption phenomena, it may be conveniently used to estimate the maximum uptake of dyes from experimental data. According to this model, Q_{eq} is related to Q_{max}, the maximum dye adsorption capacity, by the following equation:

$$Q_{eq} = Q_{max}\frac{K_L C_{eq}}{1 + K_L C_{eq}} \quad (4)$$

where K_L (L/mmol) is the Langmuir constant and represents the affinity between the sorbent active sites and the adsorbate. Langmuir parameters (K_L and Q_{max}) and the correlation coefficients are listed in Table 3. The R^2 values show that experimental data are well described by the Langmuir model. It means that even if different active sites are available in our system, they act as a homogeneous surface. On the other hand, it is consistent with the formation of a monolayer or less of dye molecules on the binding sites of the beads.

Non-encapsulated AC can adsorb the both dyes regardless of their charge; Q_{max} values have the same order of magnitude for both dyes (0.86 mmol/g_{AC} for MO and 0.62 for MB), the amount of adsorbed MO being slightly higher than for MB. This is in agreement with the properties of a pure carbon surface; it is considered that for such a non-polar surface, the main attractive force is the π–π interaction between benzene rings, similar in both MO and MB, and the graphene structure of AC [21].

Table 3
Langmuir model parameters for the sorption of MO and MB onto non-encapsulated AC and EpiMB.

Sorbent	Dye	K_L L/mmol	Q_{max} mmol/g_{AC}	Q_{max} mmol/g	R^2
AC[a]	MO	88	0.86	–	0.996
	MB	842	0.62	–	0.990
EpiMB-3	MO	47	0.76	0.02	0.999
	MB	10	26.6	0.70	0.995
EpiMB-4[b]	MO	47	0.64	0.15	0.996
	MB	13	3.57	0.81	0.997

[a] The values reported were obtained in a previous work [15].
[b] In this synthesis, 10 times more AC were introduced in the beads.

In the case of EpiMAB-2, the sign of the charge of the dye drastically affects its adsorption behavior. The Q_{max} value for negatively charged MO adsorbed onto EpiMAB-2 (0.76 mmol/g_{AC}) is close to the Q_{max} value obtained for non-encapsulated AC (0.86 mmol/g_{AC}). On the other hand, the amount of MB adsorbed by EpiMAB-2 (26.6 mmol/g_{AC}) is higher than for non-encapsulated AC due to additional electrostatic attractions between the positive charge of the dye and negative charges of the carboxylate functions of both alginate and citrate-coated magnetic nanoparticles. These results agree with the observations of Lin et al. [18], which have studied the adsorption of several organic compounds with different charges by non-encapsulated AC and AC encapsulated in alginate beads. They observed that: (1) AC adsorbs organic compounds regardless of their charge; (2) alginate beads containing AC adsorb only positively charged and neutral compounds. Jodra and Mijangos [19] also showed that the amount of negatively charged phenolate adsorbed onto an alginate/activated carbon composite is smaller than the one adsorbed onto non-encapsulated activated carbon. It is difficult to compare the adsorption capacities of our magnetic alginate beads with those of the other systems based on biosorbents described in the literature because experimental conditions are not similar. We can however notice that our values of Q_{max} are of the same order or even superior to those given in the literature [4,10,22–24].

The evolution of Na^+ and Ca^{2+} concentrations within the beads during dye adsorption by EpiMAB-2 is reported in Figs. 4 and 5 for MB and MO, respectively. It appears that adsorption of MO is

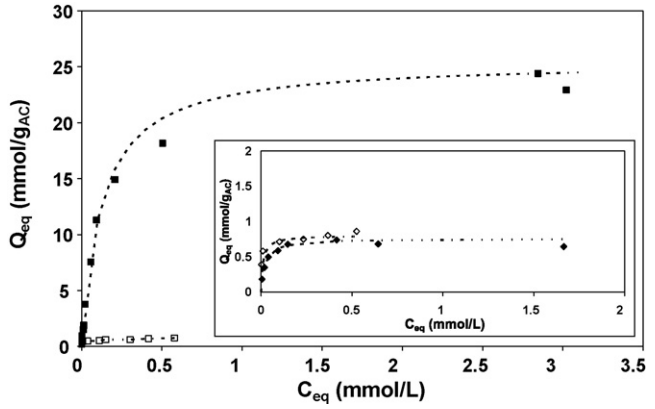

Fig. 3. Adsorption isotherms of MB onto dry EpiMB-2 (■) and non-encapsulated AC (□). Inset shows the adsorption isotherms of MO onto dry EpiMB-2 (♦) and non-encapsulated AC (◊). The dotted lines represent the fits with a Langmuir equation (pH = 7.5 ± 0.3 for MB and 8.0 ± 0.2 for MO).

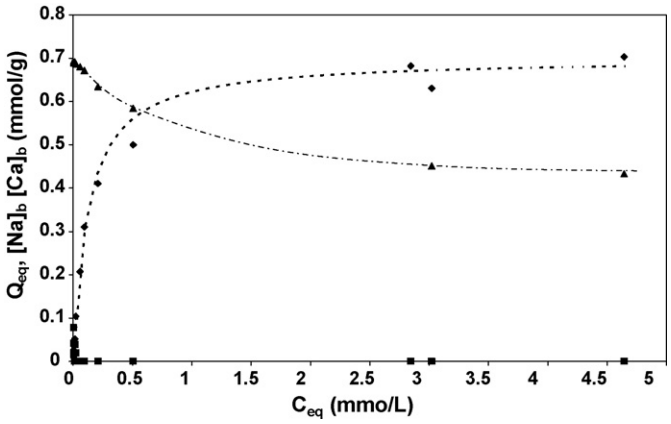

Fig. 4. Adsorption isotherm of MB onto dry EpiMB-2 and evolution of calcium and sodium contents within the beads; (♦) Q_{eq}; (▲) $[Ca^{2+}]_b$; (■) $[Na^+]_b$; dotted line represents the fit of Q_{eq} with the Langmuir equation; mixed lines are guides for eyes.

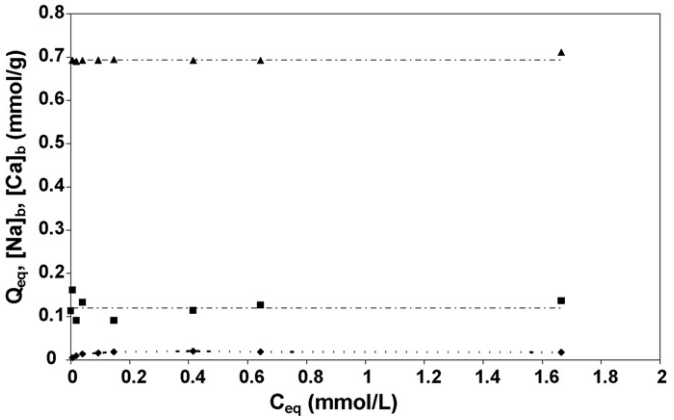

Fig. 5. Adsorption isotherm of MO onto dry EpiMB-2 and evolution of calcium and sodium contents within the beads. (♦) Q_{eq}; (▲) $[Ca^{2+}]_b$; (■) $[Na^+]_b$; dotted line represents the fit with the Langmuir equation; mixed lines are guides for eyes.

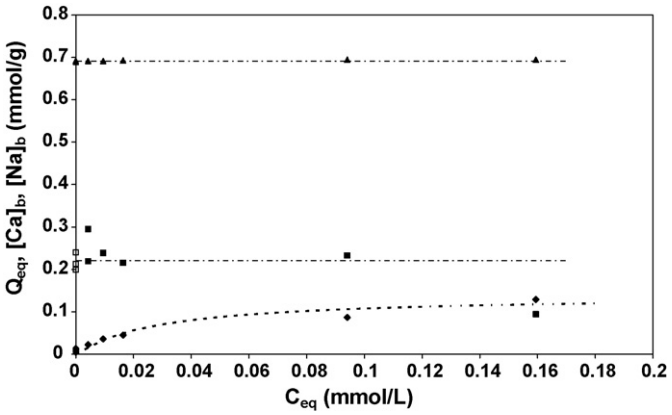

Fig. 7. Adsorption isotherm of MO onto EpiMB-3 and evolution of calcium and sodium contents within the beads. (♦) Q_{eq}; (▲) $[Ca^{2+}]_b$; (■) $[Na^+]_b$; dotted line represents the fit of Q_{eq} with the Langmuir equation; mixed lines are guides for eyes.

done without any significant change of the concentrations of Ca^{2+} and Na^+ ions within the beads. It agrees with an adsorption on encapsulated AC as it has been shown before. On the other hand, a decrease of the amounts of Ca^{2+} and Na^+ ions within the beads occurs when the amount of adsorbed MB increases. To quantify the ionic exchanges, the ratio

$$R = \frac{Q_{eq}(\text{EpiMAB}) - Q_{eq}(\text{AC})}{[M]_r} \quad (5)$$

was calculated from experimental data; Q_{eq}(EpiMAB) is the amount of MB adsorbed onto the beads, Q_{eq}(AC) is the amount of adsorbed MB onto encapsulated AC (deduced from the adsorption isotherm of MB onto non-encapsulated AC), $[M]_r = 2([Ca]_i - [Ca]_b) + ([Na]_i - [Na]_b)$ is the amount of cations released in the solution. When adsorption sites are saturated, the ratio R is close to 1 which agrees with a simple ionic exchange of MB with calcium and sodium cations.

It has to be noticed that all the calcium ions are not displaced by MB. Nevertheless, the quantity $Q_{eq}(\text{EpiMAB}) - Q_{eq}(\text{AC}) + 2[Ca^{2+}]_b + [Na^+]_b$ $(1.6 \pm 0.1\ \text{mmol/g})$ is close to the number of binding sites of the beads (1.5 mmol/g).

Adsorption experiments were also performed with EpiMAB-3 containing 10 times more AC than EpiMAB-2 (Figs. 6 and 7), the corresponding Langmuir parameters are listed in Table 3. The amounts of adsorbed dye increase with the amount of encapsulated AC, the same increase of Q_{max} between EpiMAB-2 and EpiMAB-3 is observed for both dyes: 0.13 mmol/g for MO and 0.11 mmol/g for MB. We can thus connect it with the increase of the amount of AC within the beads. As previously for EpiMAB-2, no ionic exchange with Ca and Na cations occurs during MO adsorption while concentrations of these cations within the beads decreases during MB with a ratio R close to 1.

Those adsorption experiments show that both electrostatic and hydrophobic interactions contribute to the adsorption of MB onto magnetic alginate beads; hydrophobic interactions occur with encapsulated AC and electrostatic interactions with the negatively charged sites of the beads. On the other hand, adsorption of the negatively charged MO only occurs through hydrophobic interactions. This allows for a tailoring of the selectivity of the magnetic alginate beads: the encapsulation of more AC facilitates the adsorption of dyes independently of their charge whereas an increase of the amount of alginate or magnetic nanoparticles facilitates the adsorption of positively charged dyes. These results agree with those obtained previously with CaMAB [13]. It indicates that the crosslinking of alginate with epichlorohydrin does not affect the adsorption mechanism of dye onto the magnetic alginate beads.

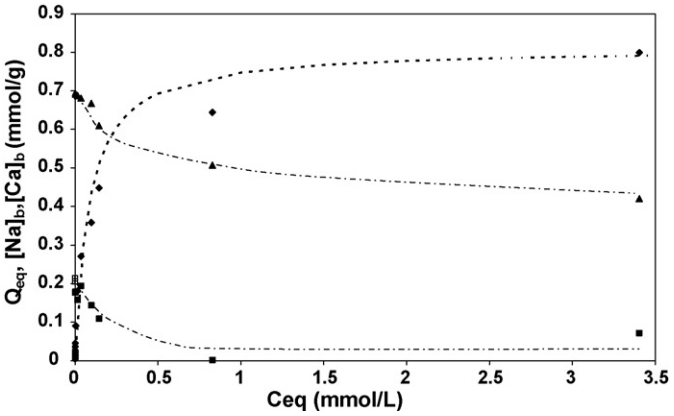

Fig. 6. Adsorption isotherm of MB onto EpiMB-3 and evolution of calcium and sodium contents within the beads; (♦) Q_{eq}; (▲) $[Ca^{2+}]_b$; (■) $[Na^+]_b$; dotted line represents the fit of Q_{eq} with the Langmuir equation; mixed lines are guides for eyes.

3.4. Effect of pH on adsorption

As we have just shown it, the adsorption of the negatively charged OM is connected to the presence of AC in beads, while carboxylate sites of the beads are involved in the adsorption of the positively charged MB. In this part, we study the effect of the variation of the quantity of carboxylate sites, occurring through pH variations, on the adsorption of MB. The effect of pH of the adsorption of MB onto EpiMAB-4 is illustrated in Fig. 8 for two MB initial concentrations (1 and 15 mmol/L), the evolution of the concentrations of calcium and sodium into the beads is also reported. At pH < 2.5, the solution takes a slight orange color due to the dissolution of the magnetic nanoparticles in Fe^{3+} ions; however, 99% of the initial magnetic nanoparticles quantity remains into the beads which thus kept their magnetic properties. The amount of calcium and sodium ions within the beads decreases with the pH according to the progressive protonation of the carboxylate functions. For C_0 = 1 mmol/L, the quantity of adsorbed MB slightly decreases for pH < 4 in agreement with an adsorption on encapsulated AC which is no-pH dependant [10,25]. On the other hand, for C_0 = 15 mmol/L, the amount of MB added is higher than the adsorption capacity of encapsulated AC, so adsorption also occurs on the carboxylate sites of the beads. In this case, the adsorbed MB quantity increases with increasing the solution pH. This is attributed to the fact that the

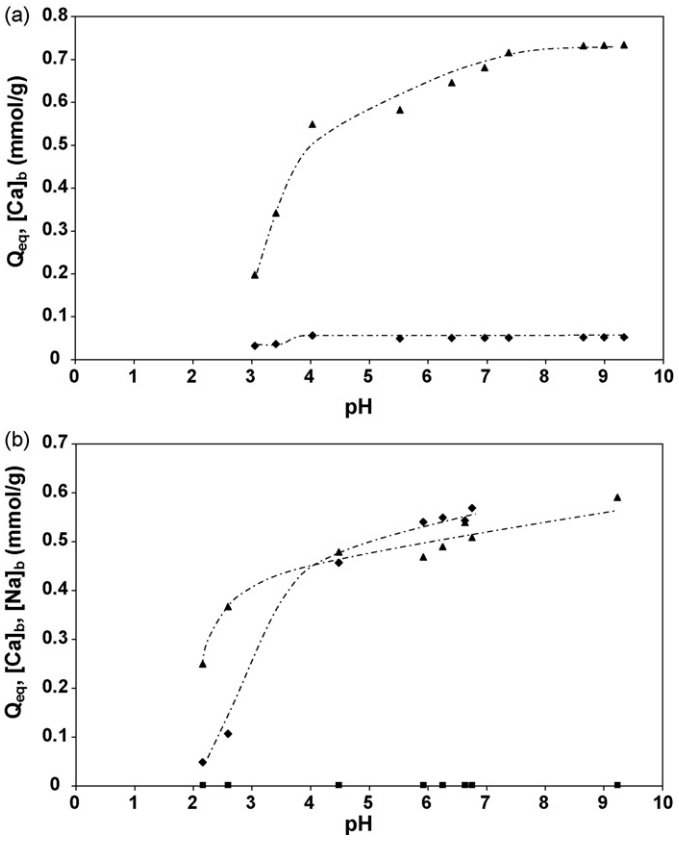

Fig. 8. Adsorption of MB onto dry EpiMB-4 and evolution of calcium and sodium contents within the beads. (♦) Q_{eq}; (▲) $[Ca^{2+}]_b$; (■) $[Na^+]_b$. Initial MB concentration: (a) C_0 = 1 mmol/L; (b) C_0 = 15 mmol/L. Mixed lines are guides for eyes.

protonation of carboxyl groups of alginate beads becomes insignificant at high pH. This behavior is in agreement with results reported in the literature [10,26,27]. Since the adsorption of MB is high at pH = 7.5, the adsorption isotherms were conducted at this pH.

4. Conclusions

In the present work an efficient magnetic biosorbent was developed by encapsulation of activated carbon and citrate-coated magnetic nanoparticles within alginate beads crosslinked with epichlorohydrin. Sorption experiments were performed using two dyes as models: negatively charged methyl orange (MO) and positively charged methylene blue (MB). Comparative kinetics experiments were conducted with alginate beads crosslinked by Ca^{2+} ions or epichlorohydrin in dry or wet state to evaluate the equilibrium time. It has been shown that the use of epichlorohydrin accelerates the adsorption even in a dry state. The pseudo-second-order kinetic model adequately describes the experimental data. At equilibrium, the adsorption behavior was well described by a Langmuir isotherm with maximum adsorption capacities equal to 0.02 mmol/g for MO and 0.7 mmol/g for MB. The influence of the pH solution on adsorption was also investigated.

In agreement with our previous results, two adsorption mechanisms were evidenced: (1) an hydrophobic adsorption onto encapsulated AC which depends neither on the electrical charge of the dye, nor of the solution pH; (2) an ionic exchange between the positively charged dye and calcium ions and sodium ions, the counterions of the carboxylate functions of both alginate and citrate-coated magnetic nanoparticles. In this case, a strong dependence with the solution occurs. These adsorption mechanisms allow monitoring the selectivity of the beads by a simple change in their formulation. Pollutants could be recovered fast and efficiently from effluents by magnetic separation.

Acknowledgements

The authors would like to express their acknowledgements to Delphine Talbot for her technical assistance. This work was done with a DGA research grant.

References

[1] M. Dogan, et al., Kinetics and mechanism of removal of methylene blue by adsorption onto perlite, Journal of Hazardous Materials 109 (1–3) (2004) 141–148.
[2] P. Liu, L. Zhang, Adsorption of dyes from aqueous solutions or suspensions with clay nano-adsorbents, Separation and Purification Technology 58 (1) (2007) 32–39.
[3] J.M. Dias, et al., Waste materials for activated carbon preparation and its use in aqueous-phase treatment: a review, Journal of Environmental Management 85 (4) (2007) 833–846.
[4] N.K. Lazaridis, et al., Chitosan derivatives as biosorbents for basic dyes, Langmuir (2007).
[5] S. Mondal, Methods of dye removal from dye house effluents. An overview, Environmental Engineering Science 25 (3) (2008) 383–396.
[6] G. Crini, Recent developments in polysaccharide-based materials used as adsorbents in wastewater treatment, Progress in Polymer Science 30 (1) (2005) 38–70.
[7] G. Crini, Non-conventional low-cost adsorbents for dye removal: a review, Bioresource Technology 97 (9) (2006) 1061–1085.
[8] F. Delval, et al., Preparation, characterization and sorption properties of crosslinked starch-based exchangers, Carbohydrate Polymers 60 (1) (2005) 67–75.
[9] J. Qu, Research progress of novel adsorption processes in water purification: a review, Journal of Environmental Sciences 20 (1) (2008) 1–13.
[10] V.J.P. Vilar, C.M.S. Botelho, R.A.R. Boaventura, Methylene blue adsorption by algal biomass based materials: biosorbents characterization and process behaviour, Journal of Hazardous Materials 147 (1–2) (2007) 120–132.
[11] A. Ayar, O. Gezici, M. Kucukosmanoglu, Adsorptive removal of methylene blue and methyl orange from aqueous media by carboxylated diaminoethane sporopollenin: on the usability of an aminocarboxilic acid functionality-bearing solid-stationary phase in column techniques, Journal of Hazardous Materials 146 (1–2) (2007) 186–193.
[12] S.-Y. Mak, D.-H. Chen, Fast adsorption of methylene blue on polyacrylic acid-bound iron oxide magnetic nanoparticles, Dyes and Pigments 61 (1) (2004) 93–98.
[13] N. Fauconnier, et al., Adsorption of gluconic and citric acids on maghemite particles in aqueous medium, Progress in Colloid & Polymer Science 100 (1996) 212–216.
[14] R. Massart, Preparation of aqueous magnetic liquids in alkaline and acidic media, IEEE Transactions on Magnetics 17 (2) (1981) 1247–1248.
[15] V. Rocher, et al., Removal of organic dyes by magnetic alginate beads, Water Research 42 (4–5) (2008) 1290–1298.
[16] G. Fundueanu, et al., Physico-chemical characterization of Ca-alginate microparticles produced with different methods, Biomaterials 20 (15) (1999) 1427–1435.
[17] G. Crini, et al., Removal of C.I. Basic Green 4 (Malachite Green) from aqueous solutions by adsorption using cyclodextrin-based adsorbent: Kinetic and equilibrium studies, Separation and Purification Technology 53 (1) (2007) 97–110.
[18] Y.-B. Lin, et al., Removal of organic compounds by alginate gel beads with entrapped activated carbon, Journal of Hazardous Materials 120 (1–3) (2005) 237–241.
[19] Y. Jodra, F. Mijangos, Phenol adsorption in immobilized activated carbon with alginate gels, Separation Science and Technology 38 (8) (2003) 1851–1867.
[20] Y.S. Ho, G. McKay, Sorption of dye from aqueous solution by peat, Chemical Engineering Journal 70 (2) (1998) 115–124.
[21] F. Villacanas, et al., Adsorption of simple aromatic compounds on activated carbons, Journal of Colloid and Interface Science 293 (1) (2006) 128–136.
[22] A.E. Sikaily, et al., Removal of methylene blue from aqueous solution by marine green alga *Ulva lactuca*, Chemistry and Ecology 22 (2) (2006) 149–157.
[23] E. Rubin, et al., Removal of methylene blue from aqueous solutions using as biosorbent *Sargassum muticum*: an invasive macroalga in Europe, Journal of Chemical Technology and Biotechnology 80 (3) (2005) 291–298.
[24] G.Z. Kyzas, D.N. Bikiaris, N.K. Lazaridis, Low-swelling chitosan derivatives as biosorbents for basic dyes, Langmuir 24 (9) (2008) 4791–4799.
[25] K. Imamura, et al., Adsorption behavior of methylene blue and its congeners on a stainless steel surface, Journal of Colloid and Interface Science 245 (1) (2002) 50–57.
[26] Y.-C. Chang, D.-H. Chen, Adsorption kinetics and thermodynamics of acid dyes on a carboxymethylated chitosan-conjugated magnetic nano-adsorbent, Macromolecular Bioscience 5 (3) (2005) 254–261.
[27] P. Waranusantigul, et al., Kinetics of basic dye (methylene blue) biosorption by giant duckweed (*Spirodela polyrrhiza*), Environmental Pollution 125 (3) (2003) 385–392.